

Virtues and Problems of the High C-Field Cs Beam Frequency Standard

Giovanni A. Costanzo, Marco Siccardi, Viatcheslav Barychev, and Andrea De Marchi

Abstract—The high C-field Cs beam frequency standard is presently a working machine that is undergoing first evaluations. The projected 10^{-14} accuracy goal is as yet unattained, mainly because of inadequate C-field uniformity and stability. An analysis of the projected possible C-field improvements and the consequent uncertainty is here reported.

I. INTRODUCTION

SEVERAL innovations have been implemented or proposed during the last decade for the accuracy improvement of thermal beam Cs standards [1] with the aim of achieving a level of 10^{-14} or better. These innovations include optical selection and detection of atoms, ring-terminated Ramsey cavities, and full self-evaluation by processing of the information content hidden in the RF response on the tube [2], [3].

A different approach was chosen at the Politecnico di Torino, based on the high C-field concept as outlined in [4]. This concept was introduced a few years ago as a way to obtain an accuracy in the low 10^{-14} without having to be exceedingly precise in the construction, reducing the cost of the machine.

In fact, it was recognized that a significant part of the efforts usually devoted to the realization of an accurate weak C-field Cs beam standard is due to the existence of biases related to neighboring transitions, Zeeman, and microwave phase effects.

As for bias effects introduced by the multilevel nature of Cesium, the approach taken in this scheme is one in which the energy separation between adjacent levels is increased beyond concern by boosting the C-field. A similar provision is enacted at times to some extent in more traditional standards [3]. However, specifications on C-field characteristics become rapidly more stringent with increasing C-field, which typically imposes a limit for level separation in weak field schemes. By setting the field value to 82 mT, requirements on field uniformity and stability are affordable, although not trivial, because the frequency of the $m_F = -1$, $\Delta m_F = 0$ hyperfine transition is minimized (see Fig. 1). The latter becomes the clock transition, and

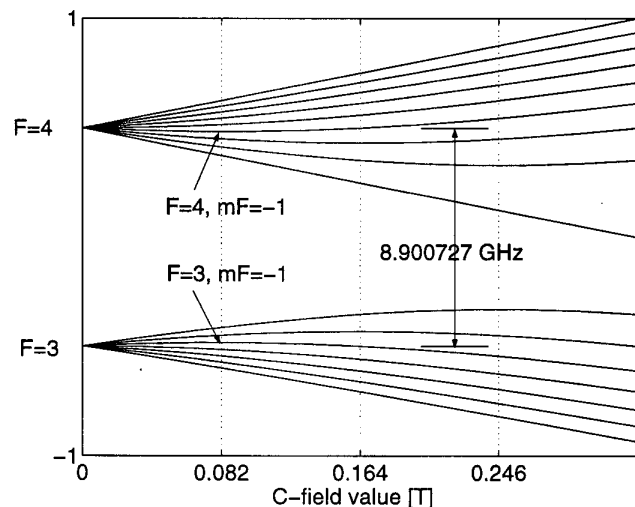


Fig. 1. Breit-Rabi law for Cs atoms.

the closest neighboring lines are some 600 MHz away from it.

Under these conditions, the first order Zeeman effect vanishes, and, from the Breit-Rabi formula, the clock frequency turns out to be

$$\nu_{-1\min} = \nu_{00} \cdot (15/16)^{1/2} \approx 8.900,727,438,257 \cdot 10^9 \text{ Hz}$$

with a residual quadratic Zeeman effect given by

$$\nu_{-1} - \nu_{-1\min} = (B - B_0)^2 \cdot 4.41 \cdot 10^{10} \text{ Hz/T}^2 \quad (1)$$

where ν_{00} is the hyperfine splitting at zero field (the SI definition of the second). Rabi and Ramsey pullings then become unimportant, as well as Majorana transitions, even with very large beam passing holes or wild spatial variations of the magnetic field.

The high value of the C-field leads naturally to a completely different design philosophy compared with other laboratory standards.

In the design that was implemented, the C-field is excited longitudinally along the beam by a solenoidal magnet [5], and the microwave transition is driven in a cylindrical multilambda Rabi cavity [6].

The chosen family of microwave modes is the $TE_{01,n}$, which features longitudinal B field on the axis and vanishing fields at the beam passing holes. This fact makes it possible to open up the holes to host a very wide beam for signal to noise ratio (S/N) maximization. A value of 10 000

Manuscript received July 12, 1999; accepted October 21, 1999. V. Barychev was supported by INFN.

G. A. Costanzo and A. De Marchi are with the Politecnico di Torino and are affiliated with the Istituto Nazionale di Fisica della Materia (INFN), Torino, Italy (e-mail: costanzo@polito.it).

M. Siccardi is with Datum-Efratom, Irvine, CA 92618-1696.

V. Barychev is with IMVP, VNIIFTRI, Mendeleev, Russia.

for the S/N was obtained with 8-mm diameter holes and 90°C Cs oven temperature.

The choice of the multilambda cavity, as opposed to a Ramsey cavity, which could still be introduced in this same apparatus whenever deemed necessary, was at first mainly driven by cost and by its superior performance with regard to end-to-end phase shift and Doppler effects [7]. However, as detailed subsequently, it turned out to be very useful in the process of assessing and optimizing C-field uniformity.

The main source of uncertainty in this Cs beam standard, in fact, comes from the limited C-field uniformity. The latter should be of the order of 10^{-6} if the corresponding bias must be kept not much greater than 10^{-14} . Correction with 10^{-14} uncertainty of the bias effect produced by a less uniform field can also be envisioned as a route to accuracy, provided the stability of the longitudinal field profile is adequate.

In the following, a quick description is given of the main features of the standard in its present configuration. An analysis of the error budget entries and a first accuracy projection are outlined in the paper.

II. DESCRIPTION OF THE APPARATUS

A. The Magnet

The prototype standard that was realized is a 1.6-m long optically pumped beam device, which has been operated in a vertical position, as shown in Fig. 2. The C-field magnet is realized with a coil of 5200 turns directly wound in 24 layers on a 60-mm i.d. Cu tube that is part of the vacuum chamber. A multilambda Rabi cavity is placed within.

Stringent specifications are imposed on the C-field for accuracy in the low 10^{-14} : uniformity and stability must approach the 10^{-6} level. An initial 10^{-3} relative spatial C-field uniformity was first measured, after assembly, along the magnet's central 40 cm. An NMR probe with 30-nT resolution was used for this purpose. An additional winding layer, tapped at each turn, was then placed around the main coil, outside a water flow cooling jacket, for successive rough uniformity optimization.

The main excitation current (about 9A) is stabilized to a few parts in 10^7 by a control loop that locks the voltage drop, produced by this current across a manganin resistor [8], to an LTZ1000 voltage reference. Servo loop electronics were designed carefully for minimal noise and temperature sensitivity. Manganin resistor and control electronics are both thermally stabilized to the mK by a PID controller, using Ziegler-Nichols rules for time constant optimization.

Long-term current drift control is planned, based on measurements of the field dependent $m_F = 0$ transition frequency. For this purpose, the multilambda cavity was designed by suitably choosing diameter and length to resonate at both the frequency ν_{-1} of the clock transition (in the $TE_{01,7}$ mode) and at the $m_F = 0$, $\Delta m_F = 0$ field dependent transition frequency ν_0 (in the $TE_{01,11}$ mode).

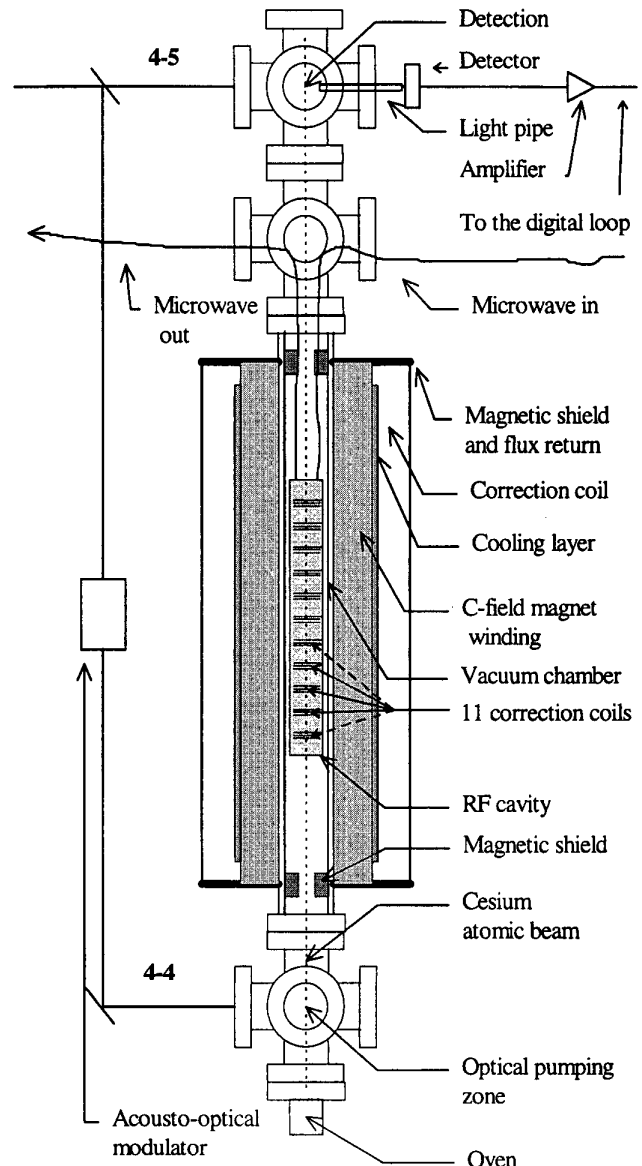


Fig. 2. Basic structure of the Cesium beam apparatus.

The current stability was confirmed by stability measurements of the standard's frequency when locked on the field-sensitive transition [9]. In medium term, the latter were consistent with the measured stability of the voltage drop across the manganin resistor. At long term, on the contrary, the two do not agree, as field stability was found worse than current stability. It turned out that such divergence is caused by temperature sensitivity of the C-field magnet. The latter was estimated with the help of a frequency vs. temperature scatter plot at a convenient field [9], which introduced some first-order field sensitivity on the clock transition.

A value close to $-10^{-4}/K$ was found for the relative temperature coefficient of the magnetic field. Temperature stabilization of the magnet to the mK level was therefore

deemed necessary. This was achieved with a digital servo control acting on the magnet's cooling water flux [9]. As a thermometer, to transduce the average temperature of the magnet winding, the coil resistance itself is used. The latter is directly measured with a volt-amperometric method.

B. The Microwave Cavity

The multilambda Rabi cavity is made of two aluminum tubes connected by a copper ring on which three semirigid coaxial cables are soldered for power input/output and terminated with two bored brass caps, which are reentrant for mode filtering.

An analysis of the cavity and related effects was carried out in several papers [6], [7], [10]. The expected residual first-order Doppler and the distributed phase shift in the multilambda cavity were shown to be consistent with the accuracy target when end cap asymmetries were no more than 1%.

C. Optical Pumping and Detection Scheme

The prototype was operated early in its life with magnetic state selection [11], [12] but was later converted to a full optically pumped scheme.

Optical pumping and detection are accomplished by using an extended cavity diode laser stabilized on the $F = 4 \leftrightarrow F' = 5$ transition of the Cs D_2 line by a saturated absorption scheme.

An acousto-optical modulator shifts the frequency of a laser beam toward the $F = 4 \leftrightarrow F' = 4$ for pumping. The fluorescent light is then imaged by two collection mirrors [13] into a light pipe passing through the vacuum wall.

D. The Frequency Chain

The microwave power is obtained by a synthesis chain: a high spectral purity BVA quartz and a 100-MHz quartz are phase locked to optimize spectral purity of the carrier [14] before frequency multiplication in a step recovery diode. A sideband of a suitable frequency, synthesized by a commercial DDS, is added in a mixer at X band to reach the clock frequency in a flexible way.

The synthesizer is square wave frequency modulated at 1 Hz for synchronous detection, and its central frequency is steered by the PC-based digital servo loop. The power stability of the microwave signal in this open loop configuration is better than one-tenth of a decibel medium term when optimized, and the spectral purity is well below concern.

III. C-FIELD-RELATED PROBLEMS

Ramsey-like patterns of the clock transition obtained with the multilambda cavity are shown in Fig. 3: high asymmetries in the shape (upper curve) are obtained with the initial 10^{-3} C-field nonuniformity. Together with this distortion, high microwave power sensitivity is also induced by field nonuniformity. Both effects are highly enhanced when the C-field value is not exactly set to

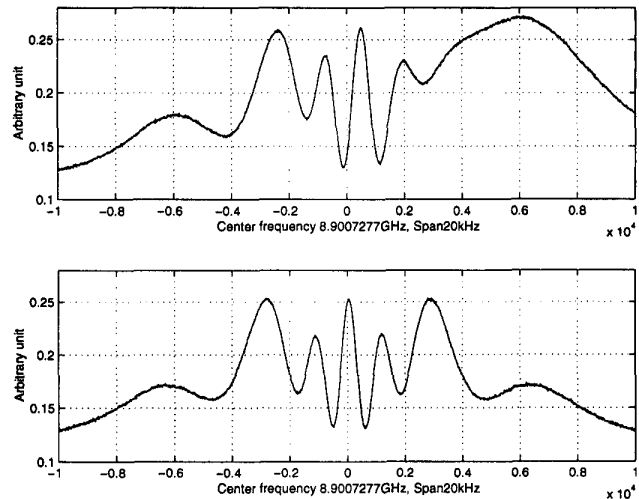


Fig. 3. Ramsey-like patterns in the multilambda cavity (span is 20 kHz). C-field relative uniformity is 10^{-3} (upper curve) and $6 \cdot 10^{-5}$ (lower curve) at 82 mT for $m_F = -1$ clock transition (center frequency is 8.900727 GHz; span, 20 kHz).

the Breit-Rabi minimum. When better magnetic uniformity is achieved by using shim coils, the resonance pattern becomes more symmetric (lower curve), and microwave power sensitivity decreases. A linewidth of 300 Hz (FWHM) for the central fringe is then obtained at a microwave power level 3 dB below optimum, in good agreement with theory [6].

Because of the low initial C-field uniformity, an improvement of three orders of magnitude was targeted to reach the desired uniformity, which was necessary for the projected accuracy of the standard.

A rough adjustment was first accomplished with the external coils by optimizing the symmetry of the clock transition's Ramsey-like pattern. This is done at a field close to the Breit-Rabi minimum. In this manner, a 10^{-4} uniformity is obtained with a fast and easy on-line procedure.

For further improvement, shim coils were wound directly on the cylindrical cavity inside the vacuum chamber to introduce local short range corrections along the microwave interaction zone.

The field sensitivity of the field dependent transition can be used as an "on-line" probe for C-field uniformity. For this reason, such shim coils were placed at nodes and antinodes of the $TE_{01,11}$ mode. In fact, because the Rabi width corresponding to a lobe's length is less than 10 kHz and because the field sensitivity is 6.8 GHz/T, a field difference of 10^{-5} between two lobes is sufficient to make them act as independent Rabi interaction zones. Their effective quantization magnetic field is locally defined for each as some power weighted average of the field distribution along the 3.5 cm of the half wavelength.

When the uniformity is worse than 10^{-5} , the multilambda Rabi cavity, therefore, provides a very effective tool for an on-line uniformity improvement procedure. In fact, the range of action of inner shim coils matches the half

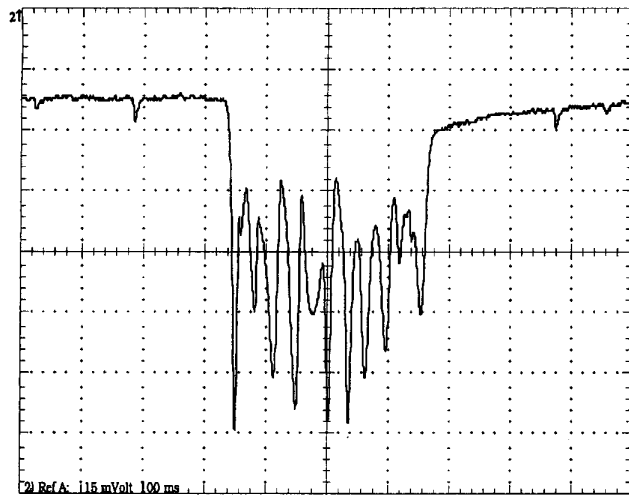


Fig. 4. The 11 Rabi resonances are shown, separated by a field with an intentional longitudinal gradient. The n th peak corresponds to the n th lobe of the $TE_{01,11}$ mode in the multilambda cavity (1.2 MHz span).

wavelength, and each separated Rabi line responds separately to a variation of the corresponding shim current.

By varying the shim currents while locking on a scope at the field dependent transition's lineshape, the 11 Rabi lines can be brought closer together, and the field uniformity can be improved as a consequence.

The sketched on-line optimization procedure works nicely until all of the Rabi lines are brought to coalesce into a single resonance, at which point they all interact, and improvements become more difficult, although possible.

Fig. 4 shows the 11 ordered Rabi lines corresponding to the 11 half wavelengths of the $TE_{01,11}$ mode when shim currents are set to induce a longitudinal field gradient sufficient to separate them.

The 20 kHz (FWHM) linewidth resonance shown in Fig. 5 was achieved [15] by using just the 11 shim coils placed at the antinodes. Shim coils positioned at the RF field nodes were added later.

IV. ACCURACY PROJECTIONS AND FREQUENCY STABILITY

A. Magnetic Field Uniformity and Stability

C-field-related problems are the main source of uncertainty for the accuracy budget because, even if the field is at the Breit-Rabi minimum, the frequency shift caused by the magnetic nonuniformities is the biggest effect.

If the FWHM of the field-dependent transition shown in Fig. 5 is used to evaluate nonuniformity, the latter is inferred to be greater than $2 \mu\text{T}$. According to (1), a frequency shift of 0.2 Hz is then expected.

As it turns out, frequency measurements of the ν_{-1} clock transition vs. a commercial frequency standard show a shift of 1.2 Hz from the calculated minimum. This

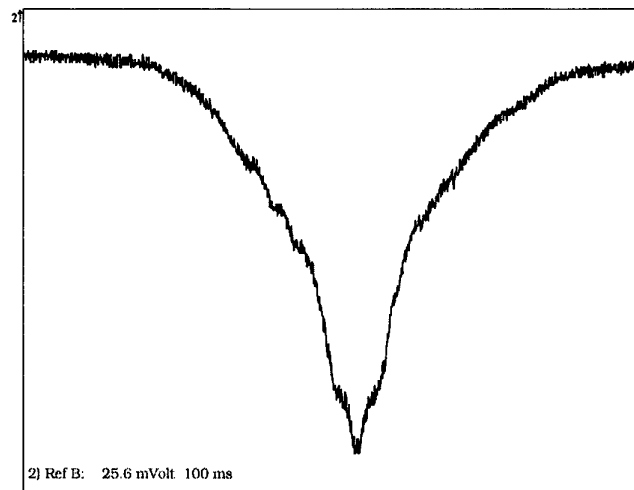


Fig. 5. $mF = 0$ field dependent transition at 82 mT (100-kHz span) after uniformity optimization.

would correspond to an rms magnetic field disuniformity of $\delta B/B = 6 \cdot 10^{-5}$, which would agree with the observed width of the ν_0 transition at its base (60 kHz). It is clear that, for an accurate prediction of this shift, the line width is not sufficient: the whole field profile should, in fact, be used as an input to a numerical step-by-step solution on the atomic systems quantum evolution [6].

Because of the limited knowledge of the actual field profile, the accuracy is presently limited to 10^{-10} by this effect, as the measured 1-Hz shift could not be explained. However, if a Ramsey-like pattern were eventually obtained in the ν_0 line shape, uniformity well below 10^{-6} would then be automatically guaranteed, and a step in accuracy of four orders of magnitude could be obtained without calculations and corrections.

Ultimately, the stability of C-field uniformity is the limit. In the existing magnet, the latter may be a potential problem. In fact, instability of the winding resistance is observed.

In Fig. 6, Allan deviation stability plots are shown for the excitation current I (with the current loop closed), the average magnetic field B (both in open and closed temperature loop), and the coil resistance R (also in both open and closed temperature loop).

It can be noticed that R is stabilized by the temperature loop. This obviously is expected because R serves as the loop sensor. Nevertheless, depending on the reasons why R changes, the C-field uniformity may still fluctuate even if R is made stable. This would be the case, for example, if R variations were driven by varying current leaks within the coil.

What appears to be a random walk process for the coil resistance, at the relative level of $7 \cdot 10^{-7} \tau^{1/2}$ (Fig. 6), could then be the signal of an instability in field uniformity, which may be very difficult to correct. However, it is hard at this point to make conjectures on the causes of this phenomenon, which may also be related to other reasons,

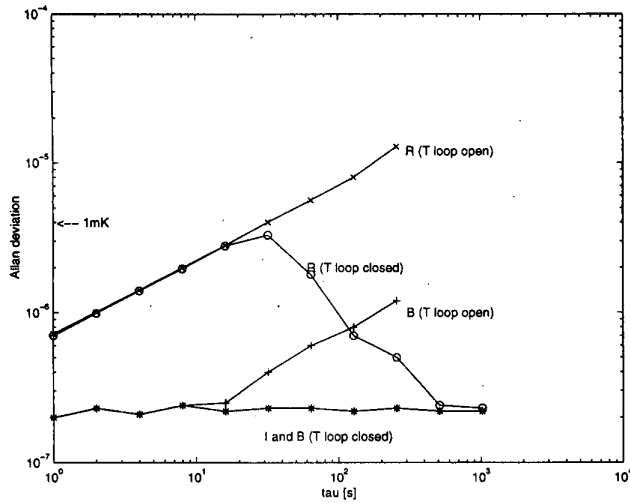


Fig. 6. Stability of the excitation current I (with the current loop closed) of the average magnetic field B (both in open and closed temperature loop) and of the coil resistance R (also in both open and closed temperature loop).

for example to varying strain gauge effects along the wire, in relation to stick-slip phenomena in mechanical stress relaxation processes. If this were the case, field uniformity would not be affected.

What unfortunately seems to be happening to the magnet is that the level of this unexplained resistance random walk process slowly gets worse as time passes, which could be an indication that something in the magnet is deteriorating.

B. Frequency and Microwave Power Stabilities

A digital servo loop with square wave frequency modulation is used for the main frequency control. The frequency of the standard is compared with that of a high spectral purity BVA quartz oscillator with a flicker floor of $2 \cdot 10^{-13}$ out to a thousand seconds. Short-term stability of the clock is $6 \cdot 10^{-12} \tau^{-1/2}$ with a Cs oven temperature of 90°C .

In Fig. 7, this effect appears particularly obvious when the frequency stability of the standard in two different power stability conditions is compared. In one case, the power had a $3 \cdot 10^{-2}$ dB $\tau^{1/2}$ superimposed random walk process, which was absent in the other case. Power sensitivity was $10^{-11}/\text{dB}$. The latter is sensitive to C-field uniformity, decreasing when uniformity improves, and is induced by the varying fashion in which the C-field is averaged, according to power. The quoted sensitivity was obtained with a uniformity of a few parts in 10^5 .

C. Cavity Pulling

No comprehensive theory exists for the cavity pulling effect in the multilambda Rabi cavity; therefore, it will have to be evaluated by cavity mistuning measurements, at least until such theory is elaborated.

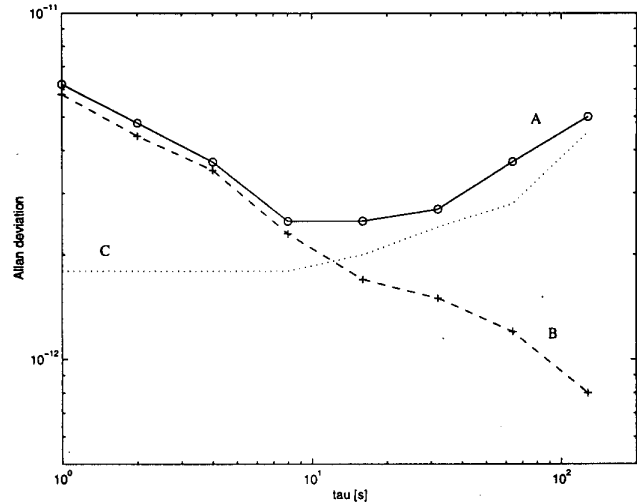


Fig. 7. Allan deviation $\sigma_y(\tau)$ for the high C-field frequency standard. Full line (A) and dashed line (B) are worst and best stability results. Dotted line (C) shows the expected effects of measured microwave power instability, calculated assuming a $10^{-11}/\text{dB}$ sensitivity coefficient.

Because of the high Q of the mode used ($\sim 10^4$), the latter can make a contribution to the standard's temperature sensitivity as large as $\Delta\nu/\nu = 2 \cdot 10^{-12}/\text{K}$, for a mistuning of a fraction of the cavity resonance width, with the assumption that the size of the effect be similar to the usual case. However, the high intrinsic Q was looked for, because it guarantees a very flat phase map, in the transversal plane, around the symmetry axis; lowering the effective Q by external loading is not an option in this configuration because of the field distortions that it induces.

A reason for optimism is the fact that the cavity temperature stability is greater than 1 mK, and, hence, its resonance frequency is stable to 200 Hz. This would generate a frequency stability limit in the low 10^{-15} , without considering the contribution of microwave power instability. The latter can be neglected when an active loop is used to stabilize microwave power fluctuations.

Because the temperature itself can be used to tune the cavity, both the cavity pulling bias and its power-induced instability can be expected to be controllable to 10^{-14} .

D. Other Shifts

It is assumed here that other frequency shifts, not directly addressed in this paper, do not contribute uncertainties above 10^{-14} . The most critical of these may be the second-order Doppler effect. However, it is assumed here that proper knowledge of the velocity distribution allow reduction of the related uncertainty below the target even with the multilambda Rabi cavity.

No consideration is given in this paper to uncertainties deriving from light shift and high-order correction terms to the Breit-Rabi formula. The former is expected not to be worse here than in other optically pumped devices, and possibly less important, because of the huge magnetic field difference between interaction zones with light and with

microwaves. The latter is expected from calculations [16] to introduce a bias at the 10^{-12} level, which is not well known, but certainly extremely stable.

V. CONCLUSIONS

Different approach routes can and have been taken toward the optimization of accuracy in Cs beam frequency standards. Each leads to a different design philosophy and a different set of relevant uncertainties [1]. In this paper, the high C-field approach was discussed with reference to the Cs beam frequency standard that was realized at the Politecnico di Torino. The prototype was described, and an analysis was made of possible contributions to the error budget.

The main source of uncertainty in this scheme is the bias determined by C-field nonuniformities, which is the only limitation down to accuracy levels in the low 10^{-14} . The virtue of this scheme is in the fact that any improvement in C-field uniformity bears directly on accuracy. In other approaches, the balance of various inaccuracy contributions is usually optimized (if the standard is fully developed), so that any design variation aimed at improving one contribution is likely to affect other contributions. Problems that still plague the efforts to reach the necessary field uniformity were illustrated.

There is, at present, a question mark on the possibility of reaching the desired field uniformity, and most of all uniformity stability, with the magnet at hand. However, the uniformity optimization procedure that was developed and illustrated here appears adequate to achieve the desired result with a suitable magnet. In such case, there shouldn't be any further obstacle toward accuracy in the low 10^{-14} .

ACKNOWLEDGMENT

The authors acknowledge useful discussions with many colleagues. Particular thanks go to R. Drullinger, G. D. Rovera, and E. Rubiola for invaluable help.

REFERENCES

- [1] A. De Marchi, "Different schemes and structure of the accuracy budget in Cesium frequency standards," in *Proc. 5th Russian Symp. Metrology of Time and Space*, pp. 102–109, 1995.
- [2] J. H. Shirley, W. D. Lee, G. D. Rovera, and R. E. Drullinger, "Rabi pedestal shifts as a diagnostic tool for primary frequency standard," *IEEE Trans. Instrum. Meas.*, vol. 44, pp. 136–139, Apr. 1995.
- [3] A. Bauch, B. Fischer, T. Heindorff, and R. Schroder, "Performance of the PTB reconstructed primary clock CS1 and an estimate of its current uncertainty," *Metrologia*, vol. 35, pp. 829–845, 1998.
- [4] A. De Marchi, "The high C-field concept for an accurate Cesium beam resonator," in *Proc. 7th EFTF*, Neuchatel, pp. 541–548, 1993.
- [5] G. Costanzo, A. De Marchi, M. Nervi, and M. Repetto, "High homogeneity solenoidal magnet for Cesium frequency standard," *IEEE Trans. Magn.*, vol. 30, no. 4, pp. 2628–2631, Jul. 1994.
- [6] A. De Marchi, P. Tavella, and E. Bava, "Multilambda Rabi cavities in atomic beam frequency standards," *J. Appl. Phys.*, vol. 82, no. 10, pp. 4711–4718, Nov. 1997.
- [7] A. De Marchi, E. Bava, and P. Tavella, "Accuracy analysis of the atom-microwave interaction in a TE_{017} cylindrical Rabi cavity for a high C-field Cesium beam resonator," in *Proc. 7th EFTF*, Neuchatel, pp. 489–493, 1993.
- [8] E. Rubiola, "High stability current control in the 10A range," *IEEE Trans. Instrum. Meas.*, vol. 45, pp. 865–871, Oct. 1996.
- [9] G. A. Costanzo, E. Rubiola, S. Therisod, M. Siccardi, F. Periale, G. D. Rovera, V. Barichev, and A. De Marchi, "The high C-field Cs beam frequency standard: present status and future improvements," in *Proc. 11th EFTF*, Neuchatel, pp. 53–57, 1997.
- [10] E. Bava, P. Tavella, and A. De Marchi, "Doppler effects in a multi-wavelength Rabi cavity for the excitation of atomic beams in microwave frequency standards," in *Proc. 46th IEEE FCS*, Salt Lake City, pp. 109–113, 1993.
- [11] G. Costanzo, M. Nervi, R. Orlando, and M. Repetto, "Design of gradient magnet system for Cs frequency standard," *IEEE Trans. Magn.*, vol. 30, no. 4, pp. 2624–2627, Jul. 1994.
- [12] G. A. Costanzo, A. De Marchi, and M. Repetto, "State selection in a bipolar gradient magnet for a high C-field Cesium beam resonator," in *Proc. 10th EFTF*, Brighton, pp. 26–29, 1996.
- [13] R. E. Drullinger, D. J. Glaze, J. Lowe, and J. Shirley, "The NIST optically pumped Cesium frequency standard," *IEEE Trans. Instrum. Meas.*, vol. 40, no. 2, Apr. 1991.
- [14] G. D. Rovera, G. Santarelli, and A. Clairon, "Frequency synthesis chain for the atomic fountain primary frequency standard," *IEEE Trans. Ultrason., Ferroelect., Freq. Contr.*, vol. 13, pp. 354–358, May 1996.
- [15] G. A. Costanzo, V. Barychev, M. Siccardi, and A. De Marchi, "On line uniformity optimization of the high C-field magnet in the Politecnico Cesium beam standard," in *Proc. 12th EFTF*, Warsaw, pp. 531–533, 1998.
- [16] W. Itano, "High magnetic-field correction to Cesium hyperfine structure," in *Proc. 5th Symp. Freq. Standard Metrol.*, Woods Hole, 1995.

Giovanni A. Costanzo was born in S. Benedetto del Tronto, Italy, on March 9, 1964. He graduated in electronic engineering from the University of Ancona (Italy) in 1989. In 1995, he received a Ph.D. in Metrology from Politecnico di Torino with a dissertation on the development and evaluation of the high C-field Cs beam frequency standard. He then went on to NRLM (Tsukuba, Japan) as a postdoctoral fellow, working on the realization of the laser system necessary for the Cs fountain. In 1998, he joined, as a permanent staff member, the Dipartimento di Elettronica at the Politecnico di Torino. Presently, he works on Cs fountain frequency standard project.

Marco Siccardi did his graduate work at the Politecnico di Torino, Torino, Italy, receiving the laurea degree in 1994 and the Ph.D. degree in 1998. During spring 1993 and summer 1994, he was at NIST, Boulder, CO, working on high performance distribution amplifiers. Since April 1999, he has been with Datum Inc., Irvine, CA. His research interests include phase noise in electronic devices for time and frequency applications and frequency synthesizers design.

Viatcheslav Barychev was born on October 5, 1956 in Baku, USSR. He graduated from Physics Department of Moscow State University in 1979.

In 1981, he joined the National Institute for Physical-Technical and Radio-Technical Measurements (VNIIFTRI), Mendeleev, Moscow, Russia, where he has been engaged in research on cesium primary frequency standards. Since 1991, he participated in the research activity of several scientific and metrological laboratories in Japan and in Italy.

His current research interests include microwave and optical frequency standards and nonlinear laser spectroscopy. He is now with the Laboratory of Atomic Frequency Standards at Politecnico di Torino, Italy.

Andrea De Marchi was born in 1947 and graduated in Electrical Engineering from the Politecnico di Torino in 1972. He has researched in the field of frequency and time metrology ever since in connection with most major metrological institutions around the world. In particular, he was with IEN in Torino for many years and spent time at the National Bureau of Standards (now NIST) in Boulder, Colorado. He is presently Professor of Electronic Measurements at the Politecnico di Torino.

His main interest is the study and improvement of atomic frequency standards, in particular based on Cesium. He was the recipient of the 1991 Rabi award for his achievements in the improvement of Cesium standards.